Published in final edited form as:
Hippocampus. 2012 August ; 22(8): 1691–1702. doi:10.1002/hipo.22004.

Temporal Manipulation of Transferrin-Receptor-1 Dependent Iron Uptake Identifies a Sensitive Period in Mouse Hippocampal Neurodevelopment

S.J.B. Fretham[1,2,3,*], **E.S. Carlson**[1,2,3,4,*], **J. Wobken**[1], **P.V. Tran**[1,2], **A. Petryk**[1,5], and **M.K. Georgieff**[1,2,3]

[1]Department of Pediatrics, University of Minnesota Medical School, Minneapolis, MN, USA

[2]Center for Neurobehavioral Development, University of Minnesota Medical School, Minneapolis, MN, USA

[3]Graduate Program in Neuroscience, University of Minnesota Medical School, Minneapolis, MN, USA

[4]Medical Scientist Training Program, University of Minnesota Medical School, Minneapolis, MN, USA

[5]Department of Genetics, Cell Biology and Development, University of Minnesota Medical School, Minneapolis, MN, 55455 USA

Abstract

Iron is a necessary substrate for neuronal function throughout the lifespan, but particularly during development. Early life iron deficiency (ID) in humans (late gestation through 2–3 years) results in persistent cognitive and behavioral abnormalities despite iron repletion. Animal models of early life ID generated using maternal dietary iron restriction also demonstrate persistent learning and memory deficits, suggesting a critical requirement for iron during hippocampal development. Precise definition of the temporal window for this requirement has been elusive due to anemia and total body and brain ID inherent to previous dietary restriction models. To circumvent these confounds, we developed transgenic mice that express tetracycline transactivator regulated, dominant negative transferrin receptor (DNTfR1) in hippocampal neurons, disrupting TfR1 mediated iron uptake specifically in CA1 pyramidal neurons. Normal iron status was restored by doxycycline administration. We manipulated the duration of ID using this inducible model to examine long-term effects of early ID on Morris water maze learning, CA1 apical dendrite structure, and defining factors of critical periods including parvalbmin (PV) expression, perineuronal nets (PNN), and brain derived neurotrophic factor (BDNF) expression. Ongoing ID impaired spatial memory and resulted in disorganized apical dendrite structure accompanied by altered PV and PNN expression and reduced BDNF levels. Iron repletion at P21, near the end of hippocampal dendritogenesis, restored spatial memory, dendrite structure, and critical period markers in adult mice. However, mice that remained hippocampally iron deficient until P42 continued to have spatial memory deficits, impaired CA1 apical dendrite structure, and persistent alterations in PV and PNN expression and reduced BDNF despite iron repletion. Together, these findings demonstrate that hippocampal iron availability is necessary between P21 and P42 for development of normal spatial learning and memory, and that these effects may reflect disruption of critical period closure by early life ID.

Corresponding Author with complete address: Michael K. Georgieff, MMC 39, 420 Delaware Street SE, Minneapolis, MN, USA, 55455, Telephone: 612 626-0644, georg001@umn.edu.
*These authors contributed equally to this study

Keywords

CA1; Transgenic tet-OFF Mouse; Iron Deficiency; BDNF; Parvalbumin

INTRODUCTION

Iron deficiency (ID) is the most common micronutrient deficiency worldwide, affecting two billion people and 20–30% of pregnant women and their offspring (Rao and Georgieff, 2007). Early life ID (late gestation through 2–3 years), results in learning and memory deficits that persist beyond the period of ID in spite of prompt iron treatment (Burden et al., 2007; Riggins et al., 2009). Long-term deficits in learning and memory following early life ID include impaired elicited imitation recall and facial recognition memory in childhood (Burden et al., 2007; Riggins et al., 2009) and impaired recognition memory performance at age 19 years (Lukowski et al., 2010), These studies suggest that iron is an important nutrient for the normal development of the hippocampus during late fetal and early postnatal life and that the neuropathology generated by reduced iron availability during that time period induces long-term behavioral abnormalities. In humans the hippocampus undergoes a period of rapid growth early in development from late gestation through the first year of life, coincident with the emergence of hippocampal-dependent recognition memory (Nelson, 1995). This period also coincides with the highest risk for early life ID in human populations (Lozoff and Georgieff, 2006).

The critical nature of iron in hippocampal development appears to stem from its role in neuronal energy metabolism through incorporation into cytochromes and intracellular globin molecules. These proteins are responsible for oxygen delivery and energy production and are highly active during periods of rapid development. Similar to humans, a period of rapid hippocampal growth and differentiation occurs early in postnatal life. In rodents, postnatal day (P)10 to P25 is characterized by profuse dendrite arborization, spine formation and synaptogenesis, and the development of characteristic adult electrophysiology (Bekenstein and Lothman, 1991a; Bekenstein and Lothman, 1991b; Pokorny and Yamamoto, 1981a; Pokorny and Yamamoto, 1981b). Energy metabolism as well as iron uptake and utilization increase rapidly in the hippocampus during this period, and are characterized by changes in ATP utilization, uptake of glucose, lactate and pyruvate, the developmental appearance of iron transport proteins, the breakdown of storage iron, and high amounts of cytochrome c oxidase activity (Blanpied et al., 2003; Cheah et al., 2006; Erecinska et al., 2004; Siddappa et al., 2002; Taylor and Morgan, 1990).

As would be expected from the human behavioral data, animal models demonstrate that the hippocampus is especially vulnerable to early life ID anemia (IDA). Rat models of early life ID are typically generated through restriction of maternal dietary iron, resulting in ID anemia in the offspring. Early life IDA results in impaired spatial learning in the water maze and win-shift radial arm maze that persists following iron repletion (Felt et al., 2006; Felt and Lozoff, 1996; Schmidt et al., 2007). In addition, formerly IDA adult rats demonstrate abnormal hippocampal electrophysiology, dendrite structure in area CA1, gene expression, and brain derived neurotrophic factor (BDNF) signaling in spite of complete iron repletion (Brunette et al., 2010; Carlson et al., 2007; Jorgenson et al., 2005; Jorgenson et al., 2003; Tran et al., 2009). Together, these observations suggest a critical requirement for iron during hippocampal development to establish normal adult structure and function.

More precise definition of the temporal window for this requirement is necessary to understand the role of iron in hippocampal development and prevent the long-term sequelae, but has been elusive due to confounders inherent to dietary IDA models. In addition to

generating total brain ID, these models render all tissues iron deficient (Dallman and Spirito, 1977; Jorgenson et al., 2003). Total body ID results in severe anemia and a prolonged repletion period of over 25 days in the rat brain once iron is reintroduced in the diet (Jorgenson et al., 2005). This lengthy repletion period corresponds to years in the developing human and is too imprecise to determine whether iron is specifically needed in the period of rapid hippocampal development.

To more precisely define the developmental window during which iron is most critical for neurodevelopment and establishment of normal adult structure and function, we developed a novel, reversible, dominant negative transferrin receptor-1 (DNTfR1) transgenic mouse model. TfR1 is the first step in neuronal iron uptake, binding diferric transferrin (Tf) and incorporating the entire complex intracellularly (Moos and Morgan, 2000). The DNTfR1 model utilizes a tissue specific conditional tetracycline responsive transgene system to reversibly over-express non-functional DNTfR1 in hippocampal pyramidal neurons (Gossen and Bujard, 1992; Mayford et al., 1996) (Fig. 1). Transferrin receptor-1 is an appealing target for the study of iron uptake by hippocampal neurons because it is preferentially targeted to dendrites coincident with the development of morphological polarity (Burack et al., 2000; Silverman et al., 2001; West et al., 1997) and is up-regulated *in vivo* in response to learning (Carlson et al., 2009). Here, we used the DNTfR1 model to manipulate TfR1 mediated iron uptake during rapid hippocampal development and demonstrated that restitution of iron uptake beginning at P21, but not as late as P42, rescues spatial learning behavior, CA1 apical dendrite structure and BDNF signaling in the adult mouse. In addition, early ID alters the number of parvalbumin (PV) positive cells and the appearance of perineuronal nets (PNN) in CA1, processes that are thought to define critical periods during development (Hensch, 2004).

MATERIALS AND METHODS

Generation of (Tet-Off) TRE-eGFP-DNTfR1 Transgenic mice

Construct Generation—Total brain RNA was isolated from C57/B6 mice and used to generate TfR1 cDNA. We generated a total brain cDNA library using oligo-dT primers from an Invitrogen reverse-transcriptase-PCR (RT-PCR) kit. We then isolated TfR1 cDNA via PCR with the forward primer 5′-CGGGATCCGATGATGGATCAAGCCAGATCA-3′ (containing a BamHI site) and the reverse primer 5′-CCATCGATGGTTAAAACTCATTGTCAATATT-3′ (containing a ClaI site). This generated a ~2.3 kb cDNA of TfR1, corresponding to its predicted size. This fragment was then ligated into pTRE2 (Clontech) using BamHI and ClaI sites. pTRE2-DNTfR1 construct was generated using site-directed mutagenesis to modify guanine[1946] to adenosine, which changes arginine[649] to histidine respectively, thus abrogating TfR1′s ability to bind transferrin ((Dubljevic et al., 1999); Fig. 1). A PCR fragment for enhanced green fluorescent protein (eGFP) was isolated using the forward primer 5′-TCCCCGCGGGGACGCCACCATGGTGAGCAAGGGA-3′ (containing a SacII site and a Kozak consensus translation initiation site) and the reverse primer 5′-CGCGGATCCGCGCCTTGTACAGCTCGTCCATGCC-3′ (containing a BamHI site and omitting the stop codon). This ~700 bp fragment was ligated into the pTRE2-DNTfR1 construct, downstream from the TRE, but upstream and in frame to the TfR-1 cDNA. The final construct (pTRE2-eGFP-DNTfR1) was linearized with a unique PvuI site for pronuclear injection. All cloning steps have been confirmed by DNA sequencing performed by the Advanced Genetic Analysis Center at the University of Minnesota.

Pronuclear injection and confirmation of genomic integration of Tg(TRE2-eGFP-DNTfR1)—The University of Minnesota Mouse Genetics Laboratory generated

founder transgenic mice positive for Tg(TRE2-eGFP-DNTfR1) by pronuclear injection. C57BL/6J female mice (21–25 days of age) were superovulated to synchronize ovulation and then mated to C57BL/6J fertile males. Fertilized embryos were collected at 0.5 days post conception. Isolated single cell embryos displaying two pronuclei were microinjected with the transgenic construct (Tg). About 22–30 injected embryos were implanted into the left oviduct of a 0.5 dpc pseudopregnant CD-1 female (6–7 weeks of age). Pups were born 19 days post implant. DNA was prepared from a tail snip for definitive genotyping by Southern blot and PCR. Genomic DNA isolated from tail snips was used to indentify the genotype of resultant offspring. Three pups positive for the Tg were unique founders; each was propagated and maintained as heterozygotes by backcrossing to WT C57BL/6J mice. Here we present findings from a single strain, *Mkg1*. Mkg1 was mated with B6;CBA-Tg(Camk2a-tTA)1Mmay/J mice (purchased from Jackson Laboratories) which express tetracycline-OFF transactivator (tTA) under the regulatory control of a CaMKIIα promoter (Mayford et al., 1996). Animals positive for DNTfR1 and Camk2a-tTA express DNTfR1 at levels sufficient to affect iron uptake, in the absence of doxycycline. Litters were generated by mating males and females positive for a single transgene with males positive for the other transgene. These doubly transgenic mice are hereafter referred to as dominant negative (DN), while offspring positive for one or no transgenes are referred to as wild type (WT) because they do not express DNTfR1.

Animal Breeding and Doxycycline Administration—All experiments were performed in accordance with the NRC's Guide for Care and Use of Laboratory Mice, and with approval of the Institutional Animal Care and Use Committee of the University of Minnesota. Mice were housed in RAR facilities in a 12 light 12 dark cycle. All experimental animals were maintained on ad lib standard laboratory chow until weaning (P21). Following weaning, animals continued on standard diet (WT^{nodox}, DN^{nodox}) or were switched to ad lib doxycycline diet (0.625mg doxycycline/kg, TD.01306, Harlan-Teklad, Madison, WI) at P21 (WT^{P21dox} and DN^{P21dox}) or P42 (WT^{P42dox} and DN^{P42dox}). The doxycycline diet was identical to the standard diet in all other nutritional aspects.

To produce animals for morphological analysis, B6;CBA-Tg(Camk2a-tTA)1Mmay/J animals were crossed with B6;Cg-Tg(Thy1-YFP)16Jrs/J animals, which expresses YFP in random subsets of neurons (Feng et al., 2000); animals positive for both transgenes were then mated with C57 BL/6-*Tg(TRE2-eGFP-DNTfR1)Mkg1* animals.

Tissue collection

Animals were euthanized by i.p. injection of Beuthanasia (10mg/kg). Whole brains used for histology were then collected following transcardial perfusion with PBS, and by perfusion with 4% PFA. Hippocampal tissue used for mRNA analysis was dissected following rapid decapitation and brain removal. Dissected hemispheres were then flash frozen in liquid nitrogen and stored at −80°C until used.

Experimental assays

Transferrin Binding—To test the ability of DNTfR1 binding to Tf in vitro, CHO cells stably expressing Tet-OFF tetracycline transactivator (CHO AA8 Tet-Off Control Cell Line, Clontech), were transfected with *Pvu*I-linearized pTRE2-pCMV:eGFP-TfR1 or pTRE2-CMV:eGFP-DNTfR1 plasmid using Lipofectamine per manufacturer's recommendation (Invitrogen). Following overnight incubation, transfected CHO cells were incubated for 1 hour with 25 μg/mL Texas-red labeled Tf (Invitrogen). Unbound Tf was removed with PBS washes. Bound Tf was visualized with light microscopy equipped with a CCD camera. Images were captured and processed using Adobe Photoshop.

Hematocrit—Trunk blood samples for hematocrit measures were taken following rapid decapitation using heparinized capillary tubes to ensure that the animals were not anemic and that doxycycline administration did not alter the hematologic status. Samples were centrifuged at 10,000 g for 10 min and hematocrit was determined using a standard hematocrit reader.

Histology—50 μm vibratome brain sections from male and female P70 WT^{nodox}, WT^{P21dox}, DN^{nodox}, and DN^{P21dox} mice were stained for storage iron using modified Perl's iron stain or mounted on slides with DAPI and imaged for CA1 apical dendrite structure as described previously (Carlson et al., 2009). Sections were imaged using a Nikon microscope (Eclipse 600) and for Perl's analysis, staining density was measured using Photoshop. Square, 20 pixel boxes were used to record the average staining intensity from a non-stained region (background) and from the CA1 pyramidal cell layer, CA3 neurons, and the cortex. Background staining intensity was then subtracted from CA1, CA3 and cortical staining intensity to determine specific regional iron staining densities as previously described (Gewirtz et al., 2008).

Immunohistological analyses for PV and PNN were performed on 20 μm frozen brain sections from male and female P30 and P70 WT, DN^{nodox}, DN^{P21dox}, and DN^{P42dox} mice not used in behavioral experiments as previously described (Balmer et al., 2009; Dityatev et al., 2007). Antigen unmasking was enhanced by pre-treating the sections with 90°C 50mM Citric acid buffer for 30 minutes before washing sections twice in Tris buffered saline (TBS) with 0.1% Triton X 100. Sections were then blocked in 10% goat serum diluted in TBS with 0.1% Triton X 100 for 30 minutes and incubated overnight at 4°C in a mixture of goat anti-parvalbumin primary antibody (1:8000, Abcam) and biotin-conjugated lectin from *Wisteria floribunda* (1:50, Sigma) diluted in blocking solution. The sections were then washed twice in TBS with 0.1% Triton X 100 and incubated with Alexa-488 goat anti-rabbit (1:200, Invitrogen) and Alexa-555 Streptavidin (1:50, Invitrogen) in TBS with 0.2% Triton X-100 for 30 minutes at room temperature. Omission of the primary antibodies as a control condition resulted in absence of staining. The sections were imaged using a Nikon microscope (Eclipse 600). The total number of PV positive cells and cells with PNNs were counted in CA1. An average of 3 sections per animal, representing an anterior, middle and posterior aspect of CA1, were assessed and averaged for each animal. Initial inspection revealed no differences in counts between the sections within each animal, confirming that there were no anterior to posterior differences in expression. Given the low number of PV positive cells expressed in hippocampus, we were able to count all of the positive cells within each section examined at a magnification that included the entire hippocampal structure.

Quantitative RT-PCR—Isolation of total RNA and qPCR was performed as previously described (Carlson et al., 2007; Tran et al., 2008). Briefly, total RNA was isolated from hippocampal hemispheres obtained from 8–10 males/group using an RNA isolation kit (Ambion). cDNA was generated using 2 μg of total RNA and a High Capacity cDNA kit (ABI). The cDNA was then diluted 10 fold. qPCR was performed in duplex using Taqman quantitative RT-PCR Universal Mix, Taqman gene expression assay probes or SYBR Green for genes of interest. The eukaryotic ribosomal protein 18S was used as an endogenous control (ABI assay 4319413E, gene accession number X03205.1). The gene expression assay probes used are described as follows (gene name, accession number, and ABI product number): *ntrk2* ($TrkB_{short}$), NM_008745.2, Mm01341751_m1; *ntrk2* ($TrkB_{long}$), NM_001025074.2, Mm01341761_m1; *bdnf* (bdnfIV), NM_001048141.1, Mm00432069_m1; *bdnf* (BDNF V), NM_001048142.1, Mm01334042_m1. SYBR Green was used to measure eGFP as a way to assess the status of the D/N gene with the following

primer set; forward primer, 5′-ACTTCAAGATCCGCCACAAC-3′ reverse primer, 5′-GTGCTCAGGTAGTGGTTGTC-3′.

Morris Water Maze—A modified version of the Morris water maze (MWM) was used to evaluate spatial memory, as previously described (Carlson et al., 2009; Choi et al., 2006). Briefly, 2–3 month old male WT $^{\text{nodox, P21dox, P42dox}}$ and DN$^{\text{nodox, P21dox, P42dox}}$ mice were tested across six consecutive days. A circular pool 120cm in diameter was filled with water occluded with white non-toxic paint and divided into virtual quadrants (NE, NW, SE, SW). A 10cm diameter escape platform was submerged 1cm below the surface in the NW quadrant. Salient visual cues were located on the walls surrounding the tank. The animals were habituated to the water on day one. During the four test days that followed animals were given five training trials with an inter-trial interval of 30 minutes. The animals were trained to search an entire quadrant for the escape platform by placing the platform in a unique position within the NW quadrant for each training trail. Animals were placed into the pool facing the wall from an entry location chosen randomly from N, NE, E, SE, S, SW positions along the pool. Animals were allowed to swim until they escaped onto the platform, if a mouse did not escape within 90 seconds, it was guided to the platform. Each of the four testing days, the animals were given a single 30 second probe trial following the training trials during which the platform was removed from the pool and the animals were allowed to swim for 30 seconds before being removed from the pool. Performance was measured by the mean escape latency and percentage of time spent in the target quadrant during training trials and by the amount of time spent searching for the submerged platform in the target quadrant during probe trials.

Visual Cued Task—On the sixth day of behavioral testing, the animals were given visual cued task (VCT) training where a visible flag was attached to the submerged platform. Animals performed three 45 second training trials. Performance was measured by escape latency as previously described (Carlson et al., 2009). The trials were video-captured and analyzed using Topscan software (Clever Systems, Reston, VA).

Data analysis

All experimental conditions consisted of DN and WT littermates from at least three independent litters. One-way Analysis of Variance (ANOVA) was used to compare staining intensity, hematocrit values, mRNA expression, and number of PV positive cells and PNNs. Two-way ANOVA was used to assess genotype × training and diet × training interactions in MWM and VCT parameters. For all analyses α was set at 0.05 and Bonferroni post-hoc analyses were used.

RESULTS

DNTfR1 expression reversibly inhibits iron uptake

To test the ability of DNTfR1 to bind transferrin *in vitro*, eGFP-TfR-1 and eGFP-DNTfR1 plasmids were transfected into Tet-Off CHO cells and incubated with Texas red labeled Tf (Texas red-Tf) (Fig. 2*A–B, D–E*). Texas red-Tf co-localized with eGFP-TfR-1 (Fig. 2*C*) but not eGFP-DNTfR1 (Fig. 2*F*).

To determine if DNTfR1 expression is sufficient to reduce *in vivo* iron uptake in the hippocampus, storage iron was analyzed with modified Perl's staining. DNTfR1 expression significantly reduces storage iron in adult DN$^{\text{nodox}}$ CA1 pyramidal neurons compared to WT$^{\text{nodox}}$ (Fig. 3*A–B,E*). Iron staining in the CA3 region and cortex is not altered in DN$^{\text{nodox}}$ mice compared to WT$^{\text{nodox}}$ littermates (Fig. 3*A–B,E*). Dietary doxycyline beginning at P21 reduces DNTfR1 mRNA expression by greater than 50% (Fig. 3*F*) and restores normal iron

status in CA1 pyramidal neurons in adult DN^{P21dox} animals (Fig. 3*C–D,E*). Iron staining in the CA3 region and cortex is not affected by doxycyline treatment (Fig. 3*C–D,E*). Therefore, DNTfR1 expression specifically and reversibly reduces iron levels in CA1 neurons without affecting iron staining in other brain regions.

DNTfR1 expression (DN^{nodox} 43.5±0.7% vs. WT^{nodox} 41.2±3.6%, p=ns) and administration of doxycycline (WT^{P21dox} 43.3±1.5% vs DN^{P21dox} 43.3±1.9%, p=ns) do not affect the hematocrit, thus assuring that the developing hippocampus is not oxygen deprived as it is in the dietary IDA models.

ID in CA1 impairs spatial memory

The effect of DNTfR1 induced hippocampal ID on spatial memory was assessed in a modified MWM task (Carlson et al., 2009; Choi et al., 2006). Adult (P70) mice WT^{nodox} mice demonstrate decreased escape latencies and spend more time in the platform quadrant across training trials (Table 1; Fig. 4*A,D* solid line). Hippocampally iron deficient DN^{nodox} mice exhibit increased escape latencies and spend less time in the platform quadrant than their iron sufficient WT^{nodox} littermates (Table 1; Fig. 4*A,D* dashed line). Additionally, DN^{nodox} animals spend more time swimming in the perimeter of the maze during training trials than WT^{nodox} littermates (Table 1; Fig. 4*G*). Consistent with performance during training, WT^{nodox} mice spent above chance amounts of time in the target quadrant across probe trials, while DN^{nodox} mice spent approximately chance amounts of time searching in the target quadrant (Table 1; Fig. 4*J*).

Iron repletion beginning at P21 but not P42 rescues learning and memory performance

Restoration of iron status began at either P21 or P42 by inhibiting DNTfR1 expression with dietary doxycycline (Fig. 3*F*). DN^{P21dox} mice showed no difference in MWM learning, characterized by reduced escape latencies and increased time spent in the platform quadrant compared to WT^{P21dox} littermates (Table 1; Fig. 4*B,E*). Furthermore, there was no longer an effect of genotype on the percentage of time spent swimming in the perimeter of the maze (Table 1; Fig. 4*H*). Ultimately, both groups demonstrated above chance amounts of time spent swimming in the platform quadrant during the probe trials (Table 1; Fig. 4*K*). In contrast, DN^{P42dox} mice showed longer escape latencies, less time spent in the target quadrant, and increased time spent swimming in the perimeter of the maze during training trials compared to WT^{P42dox} mice (Table 1; Fig. 4*C,F,I,* dashed line). Their performance was no better than DN^{nodox} mice. On the probe trials, DN^{P42dox} mice spent chance amounts of time in the platform quadrant while WT^{P42dox} littermates spent higher than chance amounts (Table 1; Fig. 4*L*).

Swim velocity and VCT performance are not affected by doxycyline or hippocampal iron status

Swim velocity and performance on a VCT assessed if DNTfR1 expression affects sensory or motor function during training. Mean swim velocity was not affected by genotype or doxycyline administration (Table 1). Three VCT trials were subsequently given to mice following completion of MWM training. There was no effect of genotype or doxycycline treatment on VCT escape latencies (Table 1). Further analysis demonstrated that doxycyline did not independently affect MWM performance within WT groups (p=0.6).

Timing of iron repletion affects dendrite structure

CA1 apical dendrite structure is an important factor associated with hippocampal learning and memory that is negatively affected by early-life ID (Brunette et al., 2010; Jorgenson et al., 2003). CA1 apical dendrites were visualized in adult (P70) mice using transgenic thy-1-

YFP In order to determine if DNTfR1-induced ID alters structure. Apical dendrites in iron deficient DN^{nodox} animals were truncated and disorganized compared to iron sufficient WT^{nodox} animals, (Fig. 5*A–B*) as previously described (Carlson et al., 2009; Jorgenson et al., 2003). Timing of iron repletion had an effect on adult apical dendrite structure. The earlier iron repleted DN^{P21dox} animals had comparable structure to always iron sufficient WT^{P21dox} (Fig. 5*C–D*), while the later iron repleted DN^{P42dox} had disrupted dendrite structure comparable to always iron deficient DN^{nodox} animals (Fig. 5*E–F*).

Early ID affects critical period markers

At P30, the number of PV positive cells and cells with PNNs in CA1 was lower in the DN^{nodox} and DN^{21dox} groups compared to WT (Fig. 6*A*) suggesting a developmental delay in the appearance of these markers. All groups had similar percentages of PV positive cells with PNNs suggesting that ID did not affect this process (Fig. 6*B*). All cells with PNNs were PV positive.

In adult mice, there were no longer any differences among groups in the number of PV positive cells in CA1 (Fig. 6*C*). However, persistent hippocampal ID in the DN^{nodox} group reduced the number of PNNs and the percentage of PV positive cells with PNNs compared to WT mice (Fig. 6*C,D*). Iron repletion at P21 in DN^{P21dox} animals restored the number of PNNs and the percentage of PV cells with nets to WT levels, however the percentage of PV cells with nets remained reduced in DN^{P42dox} animals (Fig. 6*D*). Doxycycline treatment had no effect on PV cells or PNNs in WT animals (data not shown).

Several BDNF splice variants are expressed in the adult mouse hippocampus, BDNF-IV and BDNF-V account for the majority of BDNF mRNA in the CA1 region (Malkovska et al., 2006). BDNF-V was reduced in DN^{nodox} and DN^{P42dox} mice compared to WT littermates, while there was no significant reduction in animals treated at P21 (Fig. 6*E*). Iron status has no effect on BDNF-IV mRNA levels or on expression of either the long or short isoform of the BDNF receptor TrkB (data not shown), suggesting that there is no compensatory upregulation of TrkB resulting from suppression of BDNF-V in the DN^{nodox} and DN^{P42} mice.

DISCUSSION

Using a novel approach that induces reversible and relatively specific hippocampal pyramidal cell ID, we show in this study that iron during a rapid period of hippocampal development is necessary for intact adult learning and memory performance. Previous dietary ID models result in reduced iron status of multiple brain cell populations involved in learning and memory. Thus, it is remarkable that the specific cell type manipulation of iron transport in our current model results in such a similar phenotype seen in dietary models of early ID. The findings suggest that, while not alone, pyramidal cell dysfunction contributes significantly to deficits caused by early-life ID. More specifically, our findings that iron restoration beginning at P21, but not P42, normalized learning behavior, structural and cellular signaling effects of early life ID, leads us to postulate that a developmentally critical period for iron in CA1 pyramidal neurons ends between P21 and P42. The iron sensitive time point of P21 identified in this study occurs within a period of rapid hippocampal development between P10 and P25 during which remarkable changes occur in several iron dependent processes in area CA1. These include accelerated neuronal dendrite and spine differentiation (Brunette et al., 2010; Pokorny and Yamamoto, 1981a; Pokorny and Yamamoto, 1981b), maturation of electrophysiologic capacity (Bekenstein and Lothman, 1991a; Bekenstein and Lothman, 1991b; Jorgenson et al., 2005), upregulation of synaptic plasticity genes (Carlson et al., 2007), and expression of several neurotrophic factors important for the coordination of cellular growth, including BDNF (Tran et al., 2008).

We previously isolated neuronal iron uptake as an important factor for hippocampal function and CA1 dendrite development through the generation of a pyramidal cell-specific conditional mouse knockout (CKO) of the iron transporter gene *Slc11a2,* which encodes DMT-1 protein, beginning at E 18.5 (Carlson et al., 2009; Gunshin et al., 2005). Similar to the DNTfR1 model utilized in the current study, DMT-1 CKO restricts ID to hippocampal pyramidal neurons without anemia or total body ID. Adult, iron deficient DMT-1 CKO and DN^{nodox} mice in the present study demonstrate similar spatial memory, dendrite morphology and gene expression deficits as formerly IDA rats (Brunette et al., 2010; Carlson et al., 2007; Carlson et al., 2009; Felt and Lozoff, 1996; Jorgenson et al., 2003; Tran et al., 2009). Although these findings highlight the importance of iron for hippocampal neuronal structure and function, both DMT-1 CKO and DN^{nodox} animals are iron deficient throughout development and adulthood, making it difficult to differentiate the developmental effects of ID from ongoing ID in the adult animal.

Manipulation of the timing of iron repletion using the reversible genetic model in this study made it possible to confirm our findings in the DMT-1 CKO mouse and to determine that there is a critical requirement for proper iron status during the period of rapid hippocampal growth (P10-25). It was interesting to note the apparent tropism of the transgene for CA1. CaMKIIα-tTA and therefore DNTfR1 expression occurs in all hippocampal pyramidal neurons (Mayford et al., 1996), however we noted that iron staining was only reduced in CA1 pyramidal neurons. It is possible that these cells express DNTfR1 more strongly than other cell populations, resulting in more efficient competition with endogenous TfR1. It is also possible that other cell populations use alternative iron uptake mechanisms, such as H-ferritin (Fisher et al., 2007), but that CA1 neurons are unable to use non-TfR1 mediated iron uptake systems.

Rescue of structural and behavioral phenotypes by iron restoration beginning at P21, which is late in the traditional window of rapid hippocampal development (P10-25), supports the hypothesis that early life neuronal ID adaptively extends or delays the primary period of dendrite arborization and synaptogenesis, enabling cells to complete dendritogenesis if iron becomes available. Developmental delays may be adaptive in that they allow retention of plasticity at unexpectedly late times, thereby minimizing long-term impairment. Thus, substrate provision within an appropriate and perhaps slightly extended period, allows for recovery even beyond traditional periods of development. However, the presence of behavioral and structural deficits in DN^{P42dox} mice demonstrates that P42 is beyond the point in hippocampal development when neuronal iron repletion is no longer effective in rescuing the phenotype. The findings indicate that a critical period for iron exists during hippocampal development and that this coincides with the period of rapid morphologic development. While it is possible that the DN^{P42dox} animals may eventually recover with even greater time on the doxycyline diet, this possibility is unlikely in light of the persistent deficits observed in humans and the alterations to critical period markers observed in DN^{P42dox} animals.

Significant progress has recently been made in understanding mechanisms that regulate critical periods. The balance of inhibitory and excitatory activity is a hallmark of critical periods, and the onset and duration of critical periods have been attributed to the maturation of PV positive GABA interneurons and the formation of extracellular PNNs (Hensch, 2005). Reduced numbers of PV positive cells and PNNs at P30 in DN^{nodox} animals, immediately following the traditional window of rapid hippocampal growth, suggest that early ID delays GABA-ergic maturation. This is consistent with reduced whole brain PV mRNA expression in P12 IDA rat pups (Bastian et al., 2010). Iron repletion does not reverse these effects immediately, as there is continued reduction of CA1 PV positive cells and PNNs in DN^{P21dox} animals at P30. However, the effects of iron repletion are evident in adulthood. In

spite of no difference in the number of PV positive cells between WT and DN groups, the total number of PNNs and percentage of PV positive cells with nets continues to be lower in P70 DN^{nodox} animals with ongoing ID. These effects were eliminated following P21 iron repletion, but the percentage of PV positive cells with nets remained suppressed following P42 repletion.

BDNF plays an important role in mediating the rate of ontogeny of synaptic plasticity and critical periods during development. In the visual cortex, BDNF promotes interneuron development and chronic increases in BDNF expression result in precocious critical periods (Abidin et al., 2008; Hanover et al., 1999; Huang et al., 1999). In the current study, hippocampal BDNF-V levels in adult mice were affected by iron status during development. Expression of BDNF-V mRNA was reduced by nearly 50% in adult DN^{nodox} and DN^{P42dox} animals that also showed structural and functional deficits. In contrast, BDNF-V levels were preserved in behaviorally and structurally normal adult DN^{P21dox} animals. Furthermore, the lack of compensatory upregulation of TrkB mRNA in the DN^{nodox} and DN^{P42dox} mice suggests that, overall the signaling system is depressed. The current study definitively demonstrates that lack of neuronal iron, independent of other effects of IDA, alters BDNF and that provision of iron in a time-sensitive manner promotes normal BDNF mRNA expression. Further research will be necessary to determine specifically how iron regulates BDNF gene expression and what role BDNF has in the formation and maintenance of PNNs in the adult hippocampus.

In visual cortex and amygdala PNN formation reflects critical period closure and acquisition of adult plasticity (Gogolla et al., 2009; Gundelfinger et al., 2010). While the role of PNNs in hippocampal development is less well understood, the tight association between critical period markers, BDNF expression and persistent structural and behavioral deficits following delayed iron repletion suggests an important functional linkage.

In summary, our findings demonstrate a critical requirement for iron during the period of rapid hippocampal structural and functional development. Iron deficiency in CA1 neurons during this critical period results in reduced BDNF expression and appearance of critical period markers that likely contribute to deficits in spatial memory and apical dendrite structure. The findings presented here refine our understanding of the developmental role of iron in the brain. The DNTfR1 model can be adapted in future studies to selectively interfere with iron uptake in multiple brain regions across all stages of development and pathological conditions to explore the varying roles of iron in neurodevelopment and degeneration.

Acknowledgments

Grant Sponsor: National Institutes of Health

Grant Numbers: R21-HD054490 and R01-HD29421to M.K.G, F31-NS04876 to E.S.C, and F31-NS063667 to S.F.

References

Abidin I, Eysel UT, Lessmann V, Mittmann T. Impaired GABAergic inhibition in the visual cortex of brain-derived neurotrophic factor heterozygous knockout mice. J Physiol. 2008; 586(7):1885–901. [PubMed: 18238806]

Balmer TS, Carels VM, Frisch JL, Nick TA. Modulation of perineuronal nets and parvalbumin with developmental song learning. J Neurosci. 2009; 29(41):12878–85. [PubMed: 19828802]

Bastian TW, Prohaska JR, Georgieff MK, Anderson GW. Perinatal iron and copper deficiencies alter neonatal rat circulating and brain thyroid hormone concentrations. Endocrinology. 2010; 151(8): 4055–65. [PubMed: 20573724]

Bekenstein JW, Lothman EW. A comparison of the ontogeny of excitatory and inhibitory neurotransmission in the CA1 region and dentate gyrus of the rat hippocampal formation. Brain Res Dev Brain Res. 1991a; 63(1–2):237–43.

Bekenstein JW, Lothman EW. An in vivo study of the ontogeny of long-term potentiation (LTP) in the CA1 region and in the dentate gyrus of the rat hippocampal formation. Brain Res Dev Brain Res. 1991b; 63(1–2):245–51.

Blanpied TA, Scott DB, Ehlers MD. Age-related regulation of dendritic endocytosis associated with altered clathrin dynamics. Neurobiol Aging. 2003; 24(8):1095–104. [PubMed: 14643381]

Brunette KE, Tran PV, Wobken JD, Carlson ES, Georgieff MK. Gestational and Neonatal Iron Deficiency Alters Apical Dendrite Structure of CA1 Pyramidal Neurons in Adult Rat Hippocampus. Dev Neurosci. 2010; 32(3):238–248. [PubMed: 20689287]

Burack MA, Silverman MA, Banker G. The role of selective transport in neuronal protein sorting. Neuron. 2000; 26(2):465–72. [PubMed: 10839364]

Burden MJ, Westerlund AJ, Armony-Sivan R, Nelson CA, Jacobson SW, Lozoff B, Angelilli ML, Jacobson JL. An event-related potential study of attention and recognition memory in infants with iron-deficiency anemia. Pediatrics. 2007; 120(2):e336–45. [PubMed: 17671043]

Carlson ES, Stead JD, Neal CR, Petryk A, Georgieff MK. Perinatal iron deficiency results in altered developmental expression of genes mediating energy metabolism and neuronal morphogenesis in hippocampus. Hippocampus. 2007; 17(8):679–91. [PubMed: 17546681]

Carlson ES, Tkac I, Magid R, O'Connor MB, Andrews NC, Schallert T, Gunshin H, Georgieff MK, Petryk A. Iron is essential for neuron development and memory function in mouse hippocampus. J Nutr. 2009; 139(4):672–9. [PubMed: 19211831]

Cheah JH, Kim SF, Hester LD, Clancy KW, Patterson SE 3rd, Papadopoulos V, Snyder SH. NMDA receptor-nitric oxide transmission mediates neuronal iron homeostasis via the GTPase Dexras1. Neuron. 2006; 51(4):431–40. [PubMed: 16908409]

Choi SH, Woodlee MT, Hong JJ, Schallert T. A simple modification of the water maze test to enhance daily detection of spatial memory in rats and mice. J Neurosci Methods. 2006; 156(1–2):182–93. [PubMed: 16621016]

Dallman PR, Spirito RA. Brain iron in the rat: extremely slow turnover in normal rats may explain long-lasting effects of early iron deficiency. J Nutr. 1977; 107(6):1075–81. [PubMed: 864518]

Dityatev A, Bruckner G, Dityateva G, Grosche J, Kleene R, Schachner M. Activity-dependent formation and functions of chondroitin sulfate-rich extracellular matrix of perineuronal nets. Dev Neurobiol. 2007; 67(5):570–88. [PubMed: 17443809]

Dubljevic V, Sali A, Goding JW. A conserved RGD (Arg-Gly-Asp) motif in the transferrin receptor is required for binding to transferrin. Biochem J. 1999; 341 (Pt 1):11–4. [PubMed: 10377239]

Erecinska M, Cherian S, Silver IA. Energy metabolism in mammalian brain during development. Prog Neurobiol. 2004; 73(6):397–445. [PubMed: 15313334]

Felt BT, Beard JL, Schallert T, Shao J, Aldridge JW, Connor JR, Georgieff MK, Lozoff B. Persistent neurochemical and behavioral abnormalities in adulthood despite early iron supplementation for perinatal iron deficiency anemia in rats. Behav Brain Res. 2006; 171(2):261–70. [PubMed: 16713640]

Felt BT, Lozoff B. Brain iron and behavior of rats are not normalized by treatment of iron deficiency anemia during early development. J Nutr. 1996; 126(3):693–701. [PubMed: 8598555]

Feng G, Mellor RH, Bernstein M, Keller-Peck C, Nguyen QT, Wallace M, Nerbonne JM, Lichtman JW, Sanes JR. Imaging neuronal subsets in transgenic mice expressing multiple spectral variants of GFP. Neuron. 2000; 28(1):41–51. [PubMed: 11086982]

Fisher J, Devraj K, Ingram J, Slagle-Webb B, Madhankumar AB, Liu X, Klinger M, Simpson IA, Connor JR. Ferritin: a novel mechanism for delivery of iron to the brain and other organs. Am J Physiol Cell Physiol. 2007; 293(2):C641–9. [PubMed: 17459943]

Gewirtz JC, Hamilton KL, Babu MA, Wobken JD, Georgieff MK. Effects of gestational iron deficiency on fear conditioning in juvenile and adult rats. Brain Res. 2008; 1237:195–203. [PubMed: 18789313]

Gogolla N, Caroni P, Luthi A, Herry C. Perineuronal nets protect fear memories from erasure. Science. 2009; 325(5945):1258–61. [PubMed: 19729657]

Gossen M, Bujard H. Tight control of gene expression in mammalian cells by tetracycline-responsive promoters. Proc Natl Acad Sci U S A. 1992; 89(12):5547–51. [PubMed: 1319065]

Gundelfinger ED, Frischknecht R, Choquet D, Heine M. Converting juvenile into adult plasticity: a role for the brain's extracellular matrix. Eur J Neurosci. 2010; 31(12):2156–65. [PubMed: 20497467]

Gunshin H, Fujiwara Y, Custodio AO, Direnzo C, Robine S, Andrews NC. Slc11a2 is required for intestinal iron absorption and erythropoiesis but dispensable in placenta and liver. J Clin Invest. 2005; 115(5):1258–66. [PubMed: 15849611]

Hanover JL, Huang ZJ, Tonegawa S, Stryker MP. Brain-derived neurotrophic factor overexpression induces precocious critical period in mouse visual cortex. J Neurosci. 1999; 19(22):RC40. [PubMed: 10559430]

Hensch TK. Critical period regulation. Annu Rev Neurosci. 2004; 27:549–79. [PubMed: 15217343]

Hensch TK. Critical period plasticity in local cortical circuits. Nat Rev Neurosci. 2005; 6(11):877–88. [PubMed: 16261181]

Huang ZJ, Kirkwood A, Pizzorusso T, Porciatti V, Morales B, Bear MF, Maffei L, Tonegawa S. BDNF regulates the maturation of inhibition and the critical period of plasticity in mouse visual cortex. Cell. 1999; 98(6):739–55. [PubMed: 10499792]

Jorgenson LA, Sun M, O'Connor M, Georgieff MK. Fetal iron deficiency disrupts the maturation of synaptic function and efficacy in area CA1 of the developing rat hippocampus. Hippocampus. 2005; 15(8):1094–102. [PubMed: 16187331]

Jorgenson LA, Wobken JD, Georgieff MK. Perinatal iron deficiency alters apical dendritic growth in hippocampal CA1 pyramidal neurons. Dev Neurosci. 2003; 25(6):412–20. [PubMed: 14966382]

Lozoff B, Georgieff MK. Iron deficiency and brain development. Semin Pediatr Neurol. 2006; 13(3): 158–65. [PubMed: 17101454]

Lukowski AF, Koss M, Burden MJ, Jonides J, Nelson CA, Kaciroti N, Jimenez E, Lozoff B. Iron deficiency in infancy and neurocognitive functioning at 19 years: evidence of long-term deficits in executive function and recognition memory. Nutr Neurosci. 2010; 13(2):54–70. [PubMed: 20406573]

Malkovska I, Kernie SG, Parada LF. Differential expression of the four untranslated BDNF exons in the adult mouse brain. J Neurosci Res. 2006; 83(2):211–21. [PubMed: 16385578]

Mayford M, Bach ME, Huang YY, Wang L, Hawkins RD, Kandel ER. Control of memory formation through regulated expression of a CaMKII transgene. Science. 1996; 274(5293):1678–83. [PubMed: 8939850]

Moos T, Morgan EH. Transferrin and transferrin receptor function in brain barrier systems. Cell Mol Neurobiol. 2000; 20(1):77–95. [PubMed: 10690503]

Nelson CA. The ontogeny of human memory: A cognitive neuroscience perspective. Developmental Psychology. 1995; 31(5)

Pokorny J, Yamamoto T. Postnatal ontogenesis of hippocampal CA1 area in rats. I. Development of dendritic arborisation in pyramidal neurons. Brain Res Bull. 1981a; 7(2):113–20. [PubMed: 7272792]

Pokorny J, Yamamoto T. Postnatal ontogenesis of hippocampal CA1 area in rats. II. Development of ultrastructure in stratum lacunosum and moleculare. Brain Res Bull. 1981b; 7(2):121–30. [PubMed: 7272793]

Rao R, Georgieff MK. Iron in fetal and neonatal nutrition. Semin Fetal Neonatal Med. 2007; 12(1):54–63. [PubMed: 17157088]

Riggins T, Miller NC, Bauer PJ, Georgieff MK, Nelson CA. Consequences of low neonatal iron status due to maternal diabetes mellitus on explicit memory performance in childhood. Dev Neuropsychol. 2009; 34(6):762–79. [PubMed: 20183732]

Schmidt AT, Waldow KJ, Grove WM, Salinas JA, Georgieff MK. Dissociating the long-term effects of fetal/neonatal iron deficiency on three types of learning in the rat. Behav Neurosci. 2007; 121(3):475–82. [PubMed: 17592938]

Siddappa AJ, Rao RB, Wobken JD, Leibold EA, Connor JR, Georgieff MK. Developmental changes in the expression of iron regulatory proteins and iron transport proteins in the perinatal rat brain. J Neurosci Res. 2002; 68(6):761–75. [PubMed: 12111837]

Silverman MA, Kaech S, Jareb M, Burack MA, Vogt L, Sonderegger P, Banker G. Sorting and directed transport of membrane proteins during development of hippocampal neurons in culture. Proc Natl Acad Sci U S A. 2001; 98(13):7051–7. [PubMed: 11416186]

Taylor EM, Morgan EH. Developmental changes in transferrin and iron uptake by the brain in the rat. Brain Res Dev Brain Res. 1990; 55(1):35–42.

Tran PV, Carlson ES, Fretham SJ, Georgieff MK. Early-life iron deficiency anemia alters neurotrophic factor expression and hippocampal neuron differentiation in male rats. J Nutr. 2008; 138(12): 2495–501. [PubMed: 19022978]

Tran PV, Fretham SJ, Carlson ES, Georgieff MK. Long-term reduction of hippocampal brain-derived neurotrophic factor activity after fetal-neonatal iron deficiency in adult rats. Pediatr Res. 2009; 65(5):493–8. [PubMed: 19190544]

West AE, Neve RL, Buckley KM. Identification of a somatodendritic targeting signal in the cytoplasmic domain of the transferrin receptor. J Neurosci. 1997; 17(16):6038–47. [PubMed: 9236215]

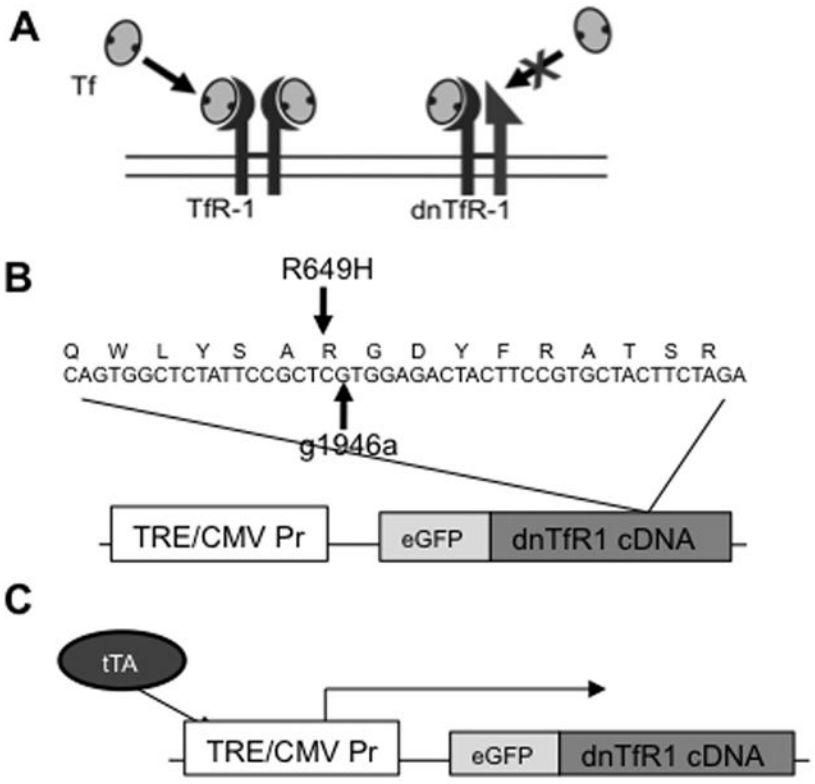

FIGURE 1. Generation of DNTfR1 transgene

(A) Schematic of DNTfR1. (B) DNTfR1 transgene contains a g1946a point mutation resulting in R649H substitution in the RGD Tf binding domain (Dubljevic et al., 1999). (C) tTA drives DNTfR1 expression from the TRE CMV promoter.

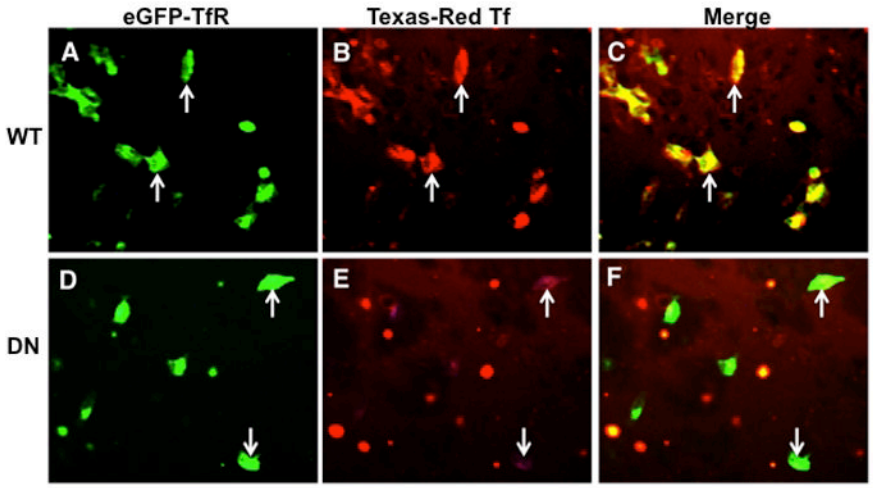

FIGURE 2. Loss of Tf binding capability in CHO cells expressing DNTfR1

Panels A–C) CHO cells transfected with high levels of eGFP-TfR (A, arrows) showing strong Tf binding (B, arrows). Merged image (C, arrows) showing extensive overlap of TfR-Tf binding in yellow. Panels D–F) CHO cells transfected with high levels of eGFP-DNTfR1 (D, arrows) showing minimal or no Tf binding (E, arrows). Trace Tf-binding is due to a small amount of residual endogenous TfR1 expression in CHO cells. Merged image (F, arrows) shows loss of TfR-Tf binding.

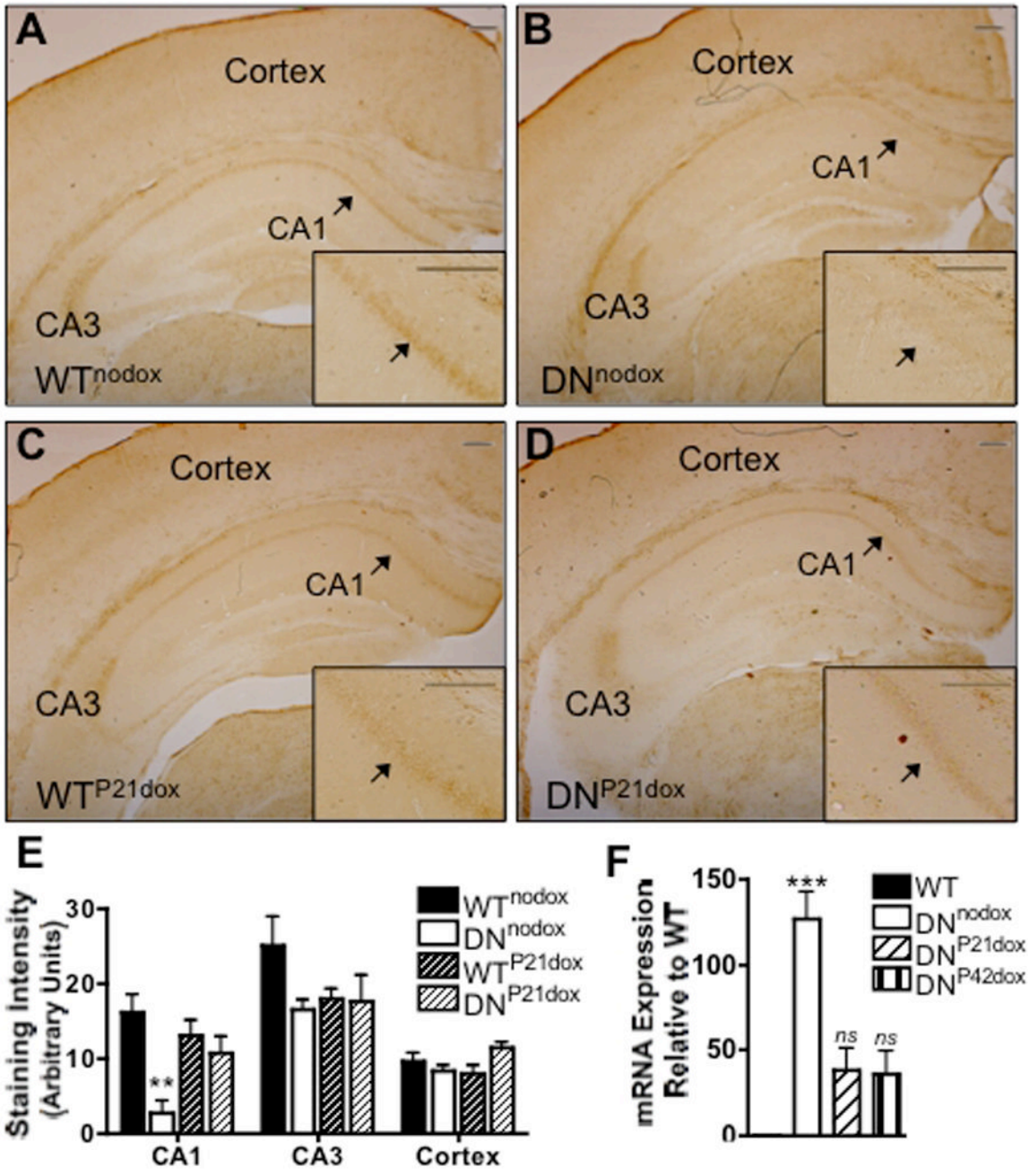

FIGURE 3. DNTfR1 expression selectively and reversibly inhibits iron uptake

in vivo. Perls' iron staining in adult hippocampus and cortex from (A) WT^{nodox} (B) DN^{nodox} (C) WT^{P21dox} and (D) DN^{P21dox} mice; inset, magnification of CA1 pyramidal cell layer indicated by arrowhead, scale bar=200 μm. (E) Quantification of staining intensity. (F) Relative expression of DNTfR1 mRNA. Data are mean ± SEM; **p<0.01, ***p<0.001

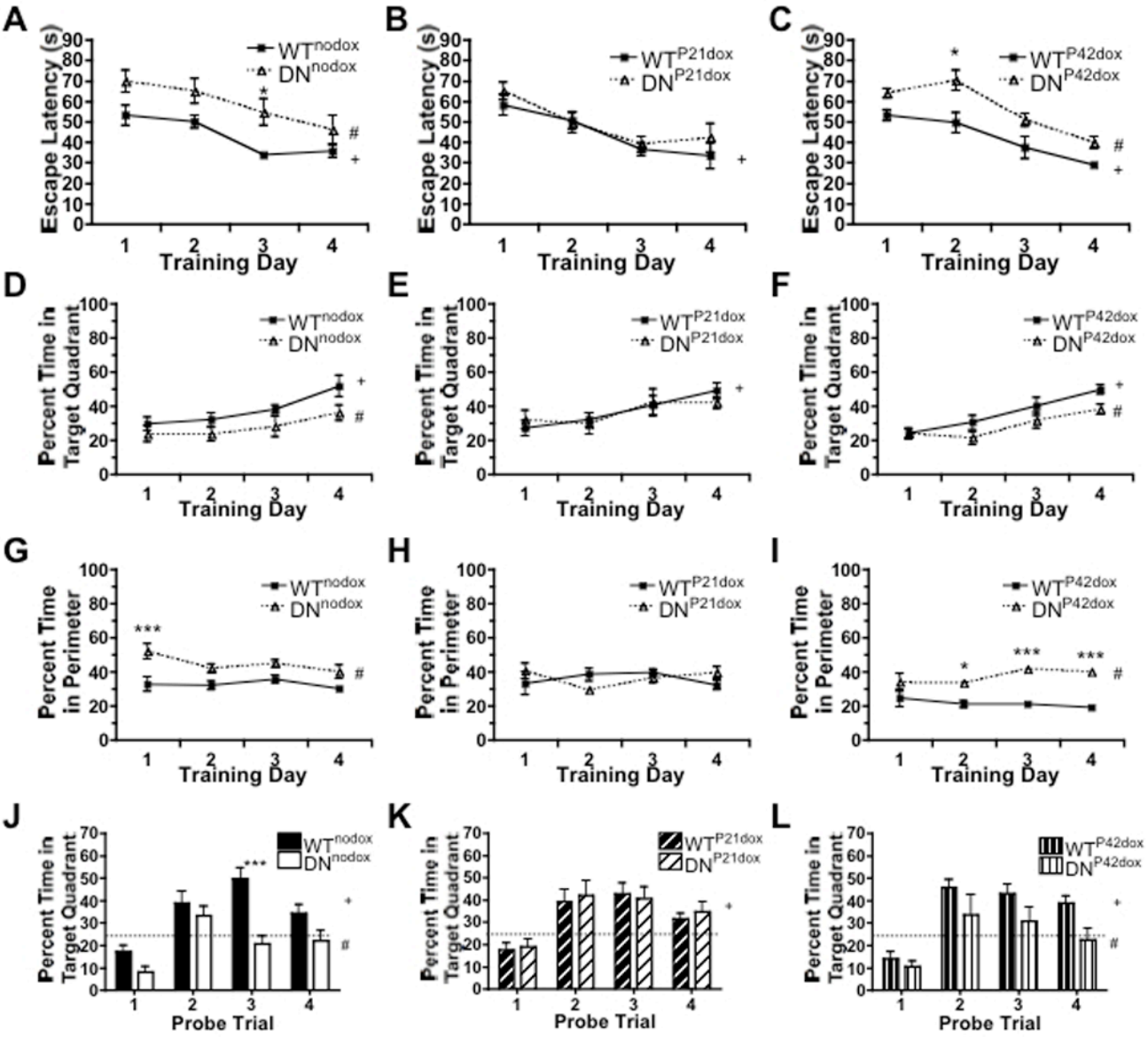

FIGURE 4. Hippocampal ID impairs spatial learning

(A–C) Average daily escape latency for (A) WT^{nodox} and DN^{nodox}, (B) WT^{P21dox} and DN^{P21dox}, and (C) WT^{P42dox} and DN^{P42dox} animals. (D–F) Average daily percentage of time spent swimming in platform quadrant during training trials for (D) WT^{nodox} and DN^{nodox}, (E) WT^{P21dox} and DN^{P21dox}, and (F) WT^{P42dox} and DN^{P42dox} animals. (G–I) Average daily percentage of time spent swimming in the perimeter of MWM during training trials for (G) WT^{nodox} and DN^{nodox}, (H) WT^{P21dox} and DN^{P21dox}, and (I) WT^{P42dox} and DN^{P42dox} animals. (J–L) Percentage of time spent target quadrant during single daily MWM probe trail for (J) WT^{nodox} and DN^{nodox}, (K) WT^{P21dox} and DN^{P21dox}, and (L) WT^{P42dox} and DN^{P42dox} animals. Data are mean±SEM (n=10–14), # indicates $p<0.05$ effect of genotype by two-way ANOVA; + indicates $p<0.05$ effect of training by two-way ANOVA; *$p<0.05$ and ***$p<0.001$ indicate Bonferroni posthoc significance.

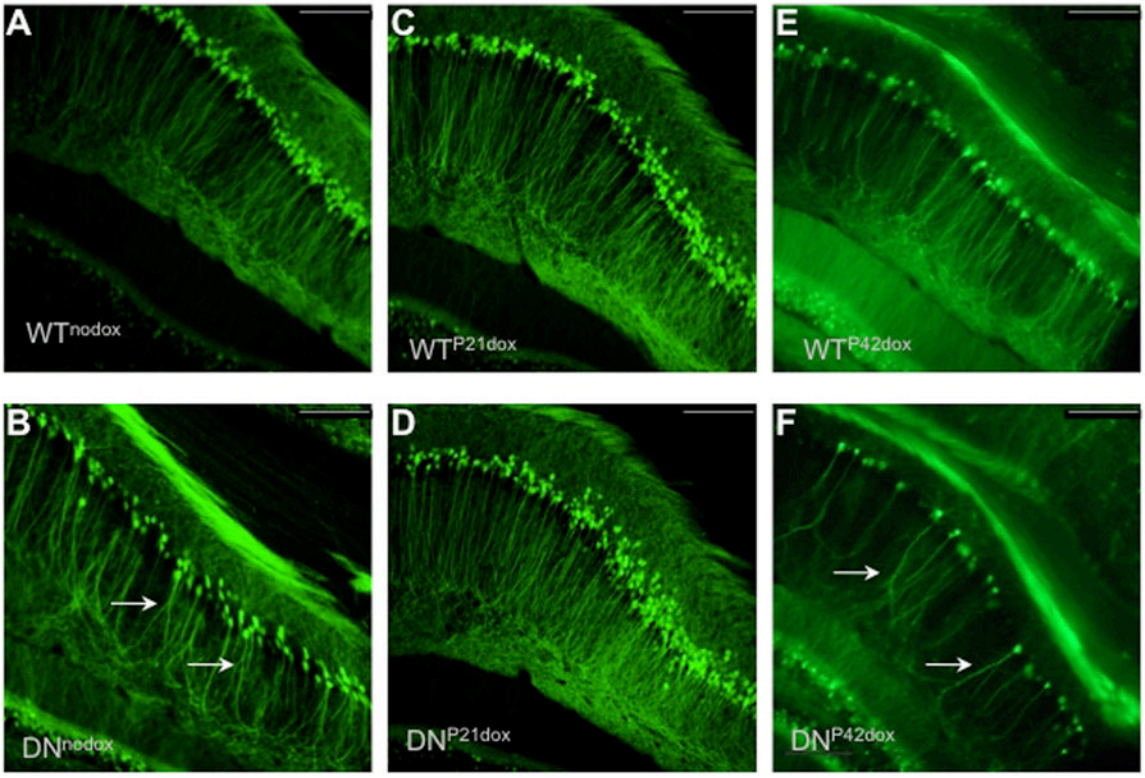

FIGURE 5. Hippocampal ID impairs CA1 apical dendrite morphology

CA1 apical dendrite morphology in (A) WT^{nodox} (B) DN^{nodox} (C) WT^{P21dox} (D) DN^{P21dox} (E) WT^{P42dox} and (F) DN^{P42dox}animals. Note the abnormal dendrite morphology (arrows) in the groups represented in Panels B and F and the lack of such abnormalities in Panel D. Scale bar=200 μm

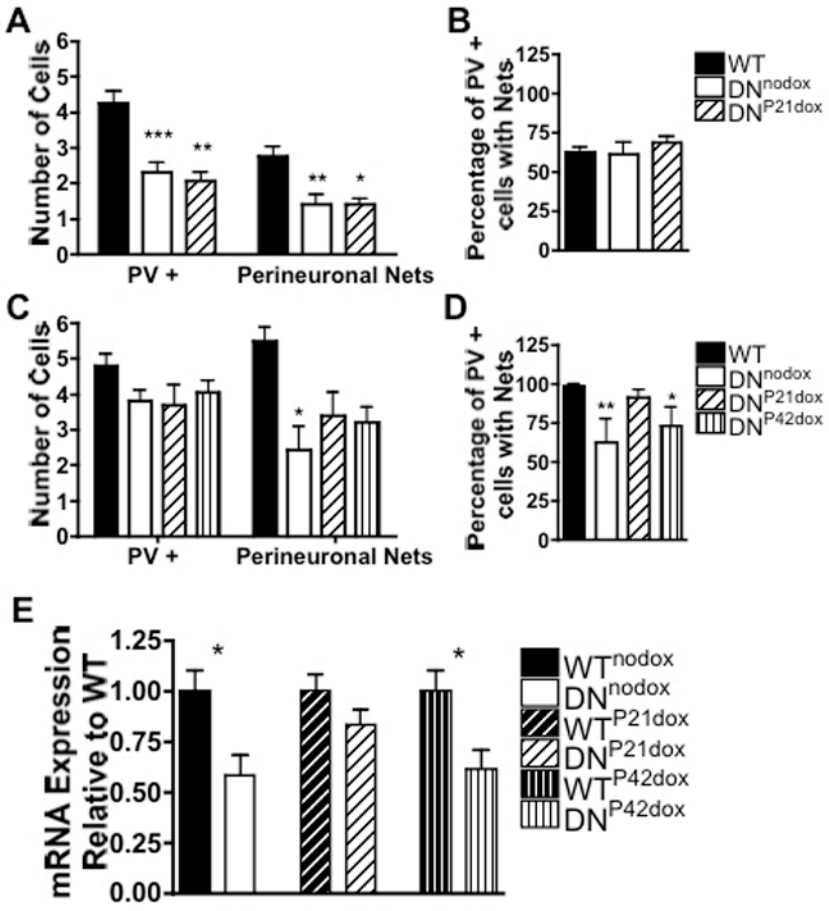

FIGURE 6. Timing of iron repletion differentially alters critical period markers and BDNF-V mRNA

Mean number of PV positive cells, PNNs and percent of PV positive cells with PNNs in CA1 of WT, DN^{nodox} and DN^{P21dox} mice at P30 (A, B) and in WT, DN^{nodox}, DN^{P21dox}, and DN^{P42dox} mice at P70 (C, D). (E) Relative expression of BDNF-V mRNA at P70. Data are mean ± SEM; *p<0.05, **p<0.01

Table 1

Statistical Analysis of MWM and VCT Performance. *p* values represent Two-Way ANOVA effects of training and genotype on MWM performance.

		No Dox (n=14,10)	P21 Dox (n=11,14)	P42 Dox (n=10,14)
		F, *p*	**F, *p***	**F, *p***
Escape Latency				
	Genotype	19.32, ***p<0.001***	1.55, *p=0.22*	29.30, ***p<0.001***
	Training	7.85, ***p<0.001***	10.62, ***p<0.001***	21.99, ***p<0.001***
Percent Time in Target Quadrant During Training				
	Genotype	9.52, ***p<0.01***	0.02, *p=0.88*	7.36, ***p<0.01***
	Training	5.63, ***p<0.01***	4.16, ***p<0.01***	12.22, ***p<0.001***
Percent Time in Maze Perimeter				
	Genotype	28.87, ***p<0.001***	0.06, *p=0.82*	57.92, ***p<0.01***
	Training	2.17, *p=0.11*	0.42, *p=0.74*	0.65, *p=0.59*
Mean Swim Velocity				
	Genotype	0.002, *p=0.96*	1.39, *p=0.24*	0.04, *p=0.85*
	Training	2.13, ***p<0.01***	1.14, *p=0.31*	1.83, ***p<0.05***
Percent Time in Target Quadrant During Probe Trials				
	Genotype	23.37, ***p<0.001***	0.13, *p=0.72*	10.62, ***p<0.001***
	Training	13.99, ***p<0.001***	9.72, ***p<0.001***	12.61, ***p<0.001***
VCT Escape Latency				
	Genotype	2.21, *p=0.14*	1.73, *p=0.19*	2.17, *p=0.15*
	Training	3.81, ***p<0.05***	1.79, *p=0.18*	0.78, *p=0.46*